

**Size and transparency influence diel vertical
migration patterns in copepods.**

Alex Barth^{*1}, Rod Johnson² and Joshua Stone¹

1. University of South Carolina, Biological Sciences, 700 Sumter St
401, Columbia, SC 29208
2. Bermuda Institute of Ocean Sciences, Bermuda GE 01, UK

² ***Scientific Significance Statement***

³ **Study Novelty**

⁴ Diel Vertical Migration is a widespread phenomenon across marine and fresh-
⁵ water systems. The predator evasion hypothesis suggests that DVM occurs as
⁶ zooplankton attempt to escape visual predators. Yet, DVM itself is a costly
⁷ and risky behavior. Thus, DVM should only occur when visual risk is high.

⁸ Several studies have shown that copepod size influences the magnitude of DVM.
⁹ However, an individual's visual risk may include traits beyond simply size. In
¹⁰ this study, we utilize an in-situ imaging tool to reveal how copepod morpholog-
¹¹ ical traits influence DVM. Our findings show that both size and transparency
¹² influence DVM. We support this finding through rigorous statistical analyses
¹³ and state-of-the-art technology. This finding provides support for leading DVM
¹⁴ hypotheses and highlights that DVM is a complex behavior driven by multiple
¹⁵ copepod traits. Furthermore, this study represents a novel application of in-situ
¹⁶ imaging technology to address major hypotheses in biological oceanography.

¹⁷ **Applicability to L&O**

¹⁸ This study addresses diel vertical migration, an active, major research topic in
¹⁹ biological oceanography. Many studies published in L&O contribute to advanc-
²⁰ ing knowledge on DVM. In this paper, we provide strong evidence for both size
²¹ and transparency influencing DVM behavior. Additionally, we accomplished
²² this study using emerging technology and statistical analyses. This work builds
²³ on research published in L&O and will be broadly applicable to plankton ecol-

²⁴ ogists, biological oceanographers.

²⁵ ***Scientific Significance Statement***

²⁶ AB and JS developed the study hypotheses. JS coordinated deployment and
²⁷ data management of the UVP. RJ facilitated data collection on cruises. AB
²⁸ led the analysis and preparation of the manuscript and figures. JS and RJ
²⁹ contributed to the manuscript draft. All authors approved the final submission.

³⁰ **Abstract**

³¹ Diel vertical migration (DVM) is a widespread phenomenon in aquatic envi-
³² ronments. The primary hypothesis explaining DVM is the predation-avoidance
³³ hypothesis, which suggests that zooplankton migrate to deeper waters to avoid
³⁴ detection during daylight. Copepods are the predominant mesozooplankton
³⁵ undergoing these migrations, however they display massive morphological vari-
³⁶ ation. Visual risk also depends on a copepod's morphology. In this study, we
³⁷ investigate hypotheses related to morphology and DVM: (H1) as size increases
³⁸ visual risk, increases in body size will increase DVM magnitude and (H2) if cope-
³⁹ pod transparency can reduce visual risk, increases in transparency will reduce
⁴⁰ DVM magnitude. In-situ copepod images were collected across several cruises
⁴¹ in the Sargasso Sea using an Underwater Vision Profiler 5. Copepod morphol-
⁴² ogy was characterized from these images and a dimension reduction approach.
⁴³ While in-situ imaging offers challenges for quantifying mesozooplankton behav-
⁴⁴ ior, we introduce a robust method for quantifying DVM. The results show a clear

45 relationship in which larger copepods have a larger DVM signal. Darker cope-
46 pods also have a larger DVM signal, however only amongst the largest group
47 of copepods and not smaller ones. These findings highlight the complexity of
48 copepod morphology and DVM behavior.

49 **Introduction**

50 Diel vertical migration (DVM) is a wide spread phenomena with large conse-
51 quences in ocean ecosystems. DVM is the process of pelagic organisms verti-
52 cally moving in the water column on a daily basis, often travelling dozens to
53 hundreds of meters (Bianchi and Mislan 2016). This large-scale event occurs
54 across many taxa, from plankton to fish (Brierley 2014). However, DVM is
55 particularly notable in zooplankton communities, whose migrations contribute
56 substantially to biogeochemical cycles (Steinberg and Landry 2017; Archibald et
57 al. 2019; Siegel et al. 2023). Mesozooplankton communities, largely dominated
58 by copepods (Turner 2004), will feed in surface layers of the ocean at night then
59 migrate into deeper waters during daytime. Through this movement, copepods
60 actively transport carbon to depth. Additionally, Kelly et al. (2019) described
61 zooplankton DVM to be a major component of mesopelagic food webs. Thus to
62 understand pelagic food webs and nutrient cycles, it is critically important to
63 understand the drivers of DVM.

64 DVM has long been studied in marine systems (Bandara et al. 2021). Predom-
65 inantly, zooplankton DVM is the movement from deep waters at daytime to

shallow waters at night (Hays 2003; Bianchi and Mislan 2016). However, reverse migration is also well documented (Ohman 1990). The adaptive benefits of DVM have been extensively reviewed (Lampert 1989; Hays 2003; Cohen and Ford Jr. 2009; Ringelberg 2009; Williamson et al. 2011; Bandara et al. 2021). Some studies have hypothesized that DVM provides a physiological advantage. It has been suggested that moving to deeper waters may provide zooplankton a reduction in UV-damage (Ewald 1912; Kessler et al. 2008), metabolic benefits (McLaren 1963; Enright 1977), or demographic benefits (McLaren 1974). However, the predator-avoidance hypothesis has received the most support to explain ultimate causes of DVM (see review of current evidence by Bandara et al. 2021). First described by Zaret and Suffern (1976), this hypothesis posits zooplankton evacuate the sunlit surface to evade visual predators then ascend at night to feed. However the massive migration undertaken by zooplankton is energetically expensive (Maas et al. 2018; Robison et al. 2020). Therefore, the predator-avoidance hypothesis makes a clear prediction that the trade-off of expended energy is worth the predator avoidance benefit (Lampert 1989). This trade-off has been further described in observations of the relationship between zooplankton feeding and DVM patterns which led to the hunger-satiation hypothesis (Atkinson et al. 1992; Pearre 2003). This hypothesis suggests that vertical migrators will ascend to feed when hungry then retreat once full. Once an individual has fully fed, remaining at the surface provides no benefit while their visual risk may increase due to their full guts which may increase visibility. Thus, the hunger-satiation hypothesis provides a detailed case of the predator-

89 avoidance hypothesis and suggests cases where copepods may forego DVM. Re-
90 gardless, both the hunger-satiation hypothesis and the predator-avoidance hy-
91 pothesis suggest DVM is primarily a result of top-down control. In modelling
92 studies with copepods, the predominant oceanic zooplankton, top-down con-
93 trol (Bandara et al. 2019) and trophic interactions (Pinti et al. 2019) have
94 successfully been used to replicate DVM patterns.

95 Predator-driven migration suggests that DVM can be a function of an individual
96 copepod's detection risk by a visual predator. However, this risk can depend on
97 a copepod's morphological features (Aksnes and Utne 1997). Notably a cope-
98 pod's size can increase visual detection. Several studies have documented that
99 copepod size influences DVM magnitude (Hays et al. 1994; Ohman and Ro-
100 magnan 2016; Aarflot et al. 2019). Presumably, a copepod's transparency will
101 also influence DVM. Hays et al. (1994) reported that pigmentation explained
102 variation in DVM frequency. However, few other studies have investigated this
103 at length. One barrier to studying a relationship between copepod morphology
104 and DVM is the difficulty of accurately recording traits. Several approaches
105 have been utilized to study DVM. High spatiotemporal resolution of DVM can
106 be achieved through acoustic (Liu et al. 2022), and even satellite-based mea-
107 surements (Behrenfeld et al. 2019). However these approaches do not yield
108 information about individuals, much less traits. Net collected specimens can al-
109 low for trait-related investigations of copepod DVM patterns (Hays et al. 1994;
110 Ohman and Romagnan 2016). However, it is much more challenging to measure
111 traits related to copepod transparency from net-collected specimens. Copepods

112 collected from deep net tows can be severely damaged and their gut contents
113 may not reflect natural conditions due to cod-end feeding or regurgitation. Fur-
114 thermore, typical preservation methods of net-specimens can result in the loss
115 of pigmentation through bleaching in ethanol or formalin or increases in opacity
116 as the copepod dies. Yet traits related to copepod's transparency are not well
117 captured in net-collected specimens which may evacuate gut contents or lose pig-
118 mentation following preservation in formalin or ethanol. In Hays et al. (1994)'s
119 investigation, the authors relied on previously published copepod carotenoid
120 values in their analyses rather than attempt to measure pigment values from
121 their preserved specimens.

122 However, these sampling challenges may be effectively circumvented with the
123 emerging use of in-situ imaging tools. By directly observing copepods, new
124 insights into their behavior and traits can be resolved (Ohman 2019). For ex-
125 ample, Whitmore and Ohman (2021) used an in-situ imaging device to describe
126 a relationship between copepod abundance with a particulate field rather than
127 chlorophyll-a. Such findings are facilitated by the fact imagery data records an
128 individual's exact position. Additionally, a copepod's true appearance, includ-
129 ing difficult to record metrics like transparency, can be measured. Thus, in-situ
130 imaging offers a new perspective to investigate DVM hypotheses. Some studies
131 observed a copepod DVM pattern with in-situ imagery data (Pan et al. 2018;
132 Whitmore and Ohman 2021). However, direct tests of DVM-related hypotheses
133 with such data have not yet been conducted.

134 In this study, we utilized in-situ imaging to evaluate how copepod morpholog-

ical traits influence DVM patterns. We specifically test the hypotheses that, (H1) as size increases visual risk, increases in body size will increase DVM magnitude and (H2) if copepod transparency can reduce visual risk, increases in transparency will reduce DVM magnitude. If these morphologically based hypotheses are true, then the larger and darker copepods will have the largest DVM magnitude.

Methods

CTD profiles and UVP imaging of copepods

Data were collected aboard the R/V Atlantic Explorer in collaboration with the Bermuda Atlantic Time-series Study (BATS) (Steinberg et al. 2001). In-situ images of plankton were acquired using an Underwater Vision Profiler (UVP5) (Picheral et al. 2010). The original sampling methodology and instrument specification followed details described in Barth and Stone (2022). The UVP was attached to the CTD rosette and deployed regularly on cruises to the Sargasso Sea from June 2019 - December 2021. Typical monthly cruises included ~13 profiles with average descents to 1200m (Supplemental Figure S1). In this study, we investigated general trends in DVM by pooling together casts across multiple cruises. This approach is necessitated by the small sampling volume of the UVP (1.1L/image) and low abundance of plankton which requires aggregation of data to resolve trends (see details in Barth and Stone 2022). While there was minor variation between cruises (Supplemental Figure S2), this oligotrophic system is

156 relatively consistent across seasons (Steinberg et al. 2001). Additionally, every
157 cruise had an approximately equal number of day and night casts. Profiles
158 were assigned to be day or night based on locally calculated nautical dawn and
159 nautical dusk times using the R package **suncalc** 0.5.1.

160 The UVP records images of large particles ($>600\mu\text{m}$ equivalent spherical diam-
161 eter, ESD). However, living particles are not reliably identifiable below $900\mu\text{m}$
162 (Barth and Stone 2022). All recorded images were processed using Zooprocess
163 (Gorsky et al. 2010), which provides several metrics related to size, grey value,
164 and shape complexity. These features were then used to automatically sort im-
165 ages using Ecotaxa (Picheral et al. 2017). All images were manually verified
166 by the same trained taxonomist. In total, 294,913 images were recorded. Of
167 these, 85.2% were images of debris or artefacts. The smallest identified copepod
168 was 0.940mm ESD and the largest was 5.904mm ESD. Across all casts, cope-
169 pods were the most common organism, composing 58.7% of all identified, living
170 particles. In total, there were 4151 individual copepods images.

171 Morphological Grouping

172 Zooprocess measures and collects several morphologically relevant parameters.
173 To create relevant groups of copepods, a dimension reduction approach was used.
174 Similar methods have been successfully utilized to provide novel insights to ma-
175 rine snow (Trudnowska et al. 2021; Szeligowska et al. 2021), copepod dynamics
176 in the Arctic (Vilgrain et al. 2021), and temporal trends in phytoplankton com-
177 munities (Sonnet et al. 2022). First, 18 morphologically relevant parameters

178 were selected to be included in a Principal Components Analysis (PCA), fol-
179 lowing (Vilgrain et al. 2021). Parameters can be described as relating to size
180 (e.g. major axis, equivalent spherical diameter [ESD]), grey intensity (e.g. mean
181 grey value at 625nm wavelength light), shape (e.g. elongation, symmetry), and
182 shape complexity (e.g. fractal dimension). Grey-value intensity specifically can
183 capture a variety of characteristics related to particle transparency (Gorsky et
184 al. 2010). Note that the UVP5 utilizes a narrow band pass filter set to 625
185 nm, removing the effect of ambient lighting on particle transparency metrics
186 (Picheral et al. 2010). Feeding these multiple metrics into a morphospace analy-
187 sis has several advantages. First, Principle Components establish the major axes
188 of variability which can aid in interpreting the relative importance of different
189 traits. Furthermore, in the context of this study, there are several factors which
190 influence copepod transparency which are not easily distinguishable in most
191 UVP images. If only one metric was selected it may only capture one aspect of
192 transparency, thus by including all factors, we can create a composite metric.
193 Such approaches have been utilized successfully to infer characteristics in in-situ
194 imaged marine snow (Trudnowska et al. 2021; Szeligowska et al. 2021).

195 The PCA was weighted by the volume sampled in a 1-m depth bin for each
196 observation. This approach provides a correction for the UVP's variable descent
197 speed which can cause duplicate imaging of individuals. While this phenomena
198 has a minor impact on overall results (Barth and Stone 2022), we used the
199 weighted approach to assure that no individual features were overrepresented.
200 All morphological descriptors were scaled and centered prior to inclusion in the

²⁰¹ analysis. The model was constructed using the R package **FactoMineR** 2.7.
²⁰² Principal Components (PCs) were deemed to be significant if their eigenvalues
²⁰³ were greater than 1. This approach yielded 4 PCs which described 87.3% of
²⁰⁴ the total variation in morphological parameters, with 34.5% and 26.5% in the
²⁰⁵ first two components respectively. The third and fourth PCs were related to the
²⁰⁶ orientation of the copepod and appendage visibility respectively. Presumably,
²⁰⁷ this is an artifact of how the copepod was imaged. Because all axes in a PCA
²⁰⁸ are orthogonal to one another, the variation captured by PC1 and PC2 are
²⁰⁹ largely spread evenly across the copepod image variability (PC3 & PC4). This
²¹⁰ is a particularly useful feature as copepod orientation presumably impacts some
²¹¹ metrics such as size and grey-value. Yet, because orientation is largely accounted
²¹² for with PC3, by grouping along the first two PCs, variation attributable to
²¹³ orientation is homogeneous across those axes.

²¹⁴ To address our morphology-DVM hypotheses, we constructed discrete morpho-
²¹⁵ logical groups based on the first two principal components. Groups along each
²¹⁶ of the principal components were defined as low (below 25th percentile), mid
²¹⁷ (25th-75th percentile) and high (greater than 75th percentile). To address the
²¹⁸ size-dependent hypothesis (H1), groups were assigned as low, mid, or high along
²¹⁹ PC1. Then to assess if color/transparency was a secondary factor (H2), within
²²⁰ each PC1 group, PC2 groups were constructed as low, mid, or high. In total,
²²¹ this created 9 groups (e.g. Low PC1-Low PC2, Low P1-mid PC2, etc).

222 **Copepod vertical structure & DVM**

223 **Vertical distribution of copepods**

224 Copepods in this system are well documented to undergo DVM (Steinberg et
225 al. 2000; Schnetzer and Steinberg 2002; Maas et al. 2018). However, there
226 have not been direct measurements of DVM with in-situ imaging data. First, to
227 assess which portion of the water column copepods were utilizing for DVM, we
228 visualized the average vertical structure. The concentrations of each morpholog-
229 ical group (based on PC1 and PC2) were calculated in 20m depth bins for each
230 UVP profile. Profiles were designated as either day or night. Then across all
231 day/night profiles, the mean concentration was calculated for each 20m depth
232 bin.

233 **Weighted mean depth variability**

234 Weighted mean depth (WMD) is a common metric to describe vertical structure
235 and DVM in zooplankton (Ohman et al. 2002; Ohman and Romagnan 2016;
236 Aarflot et al. 2019). However, with in-situ imagery and our particular dataset,
237 this approach presents a few challenges. WMD cannot be calculated individually
238 for each profile then averaged because many profiles in this study had different
239 descent depths. Additionally, the small and uneven sampling volume of the
240 UVP can make single casts too variable to reliably resolve abundance. Yet, un-
241 derstanding variation around the WMD is necessary to compare DVM strength
242 across groups. Here, we introduce a depth-bin constrained bootstrap approach
243 to define WMD with a 95% confidence interval. To do this, the concentration of

244 each group, was calculated in 20m depth bins for each profile. Then all profiles
 245 were ‘pooled’, separately for day/night. This provides a distribution of concen-
 246 trations in each depth-bin. Pooling across multiple seasons was necessary to
 247 have sufficient data, however it does introduce additionally variability. Due to
 248 the different descent speeds and depth of profiles, there are more observations
 249 of surface depth bins. Thus, traditional bootstrapping would bias estimate to-
 250 ward the surface as resampling would be more likely to draw a more-frequently
 251 observed surface bin. To avoid this, bootstrap samples were “bin-constrained”
 252 such that for each iteration, a random observation was drawn within each depth
 253 bin, then replaced for the next iteration. A maximum depth was set to 600m
 254 based on qualitative observations of vertical profiles. This approach effectively
 255 created a random profile by resampling a concentration, $conc^*$, from each depth
 256 bin, d . For each iteration, the random constructed profile then was used to cal-
 257 culate a bootstrapped weighted mean depth, WMD^* . This was done for each
 258 morphological group, g , at each time of day, t (day/night).

$$WMD_{g,t}^* = \sum_i^{N=30} \frac{d_i(conc_{i,g,t}^*)}{\sum_i^{N=30} conc_{i,g,t}^*}$$

259 The distribution of $WMD_{g,t}^*$ then was used to calculate a bootstrapped mean
 260 and 95% confidence interval. The width of the confidence interval then is influ-
 261 enced both by the spread of copepods through the water column and the amount
 262 of data available to confidently support their estimates. Thus, this resampling
 263 approach is conservative in identifying a significant trend. The conservative

²⁶⁴ approach is desirable given both its robustness to UVP sampling variability and
²⁶⁵ the need to pool casts as described above. To assess a DVM pattern, the 95%
²⁶⁶ CIs can be compared between times of day and morphological groups. We define
²⁶⁷ a clear DVM signal (e.g. significant day/night difference) as when there is no
²⁶⁸ overlap between the 95% WMD CIs between nighttime and daytime
²⁶⁹ groups. If a clear signal was observed, the DVM magnitude can be measured
²⁷⁰ by comparing the mean *WMD**s.

²⁷¹ With PC1 to assess the size-based hypothesis (H1), the WMD was compared
²⁷² between the three PC1-groups by percentile level. Then to assess the effect of
²⁷³ transparency (H2) the WMD was compared between PC2-groups within each
²⁷⁴ PC1-grouping.

²⁷⁵ Results

²⁷⁶ Morphological Groups

²⁷⁷ The PCA revealed four major axes of variability (Figure 1). The first axis (PC1,
²⁷⁸ 34.23% of variability) was largely explained by increasing values related to size,
²⁷⁹ such as perimeter (loading score = 0.927) and feret diameter (maximum distance
²⁸⁰ between parallel planes around an object) (loading score = 0.910). The second
²⁸¹ axis (PC2, 27.24% of variability) can be interpreted as a gradient of transparent
²⁸² to dark individuals. PC2 was largely anticorrelated with mean grey value (higher
²⁸³ values indicate a more transparent individual) (loading score = -0.920). As
²⁸⁴ noted in the methods, PC3 and PC4 were both related to the orientation of the

²⁸⁵ copepod and the appendage visibility respectively (Supplemental Figure 3).

²⁸⁶ The morphological groupings were assigned along PC1 as low, mid and high.

²⁸⁷ Then along PC2, groups were assigned within each PC1-group (Figure 1). To

²⁸⁸ confirm the morphospace grouping resulted in ecologically relevant categories,

²⁸⁹ the morphological groups were compared against known copepod metrics.

²⁹⁰ Across all PC1-groups, there was a clear difference in feret diameter. The

²⁹¹ median feret diameter of the low group was 1.97mm. The median feret diameter

²⁹² of the mid and high groups were 2.84mm and 4.83mm, respectively (Figure 2A).

²⁹³ All groups were significantly different from one another (Dunn Kruskall-Wallace

²⁹⁴ test, $p < 0.001$). PC2 groups as a whole were also significantly different from

²⁹⁵ one another (Dunn Krustall-wallace test, $p < 0.001$). However, within each

²⁹⁶ PC2-group, there was a clear tendency for larger copepods (high PC1 group)

²⁹⁷ to be more transparent (Figure 2B).

²⁹⁸ **Vertical Profiles of Morphological Groups**

²⁹⁹ For all groups, the 20m-binned profiles show a notable structure. While cope-

³⁰⁰ pods were observed throughout the mesopelagic (Supplemental Figure 4), the

³⁰¹ majority of day/night differences were observed above 600m (Figure 3). For

³⁰² most morphological groups, there was a peak in nighttime concentration in the

³⁰³ lower epipelagic (50m-200m). Similarly, there was a decrease in average day-

³⁰⁴ time concentration over the same region. This pattern is particularly apparent

³⁰⁵ for the groups which are mid and high on both PCs (Figure 3B, C, E, F). Across

³⁰⁶ all groups, both average daytime and nighttime concentration were low in the

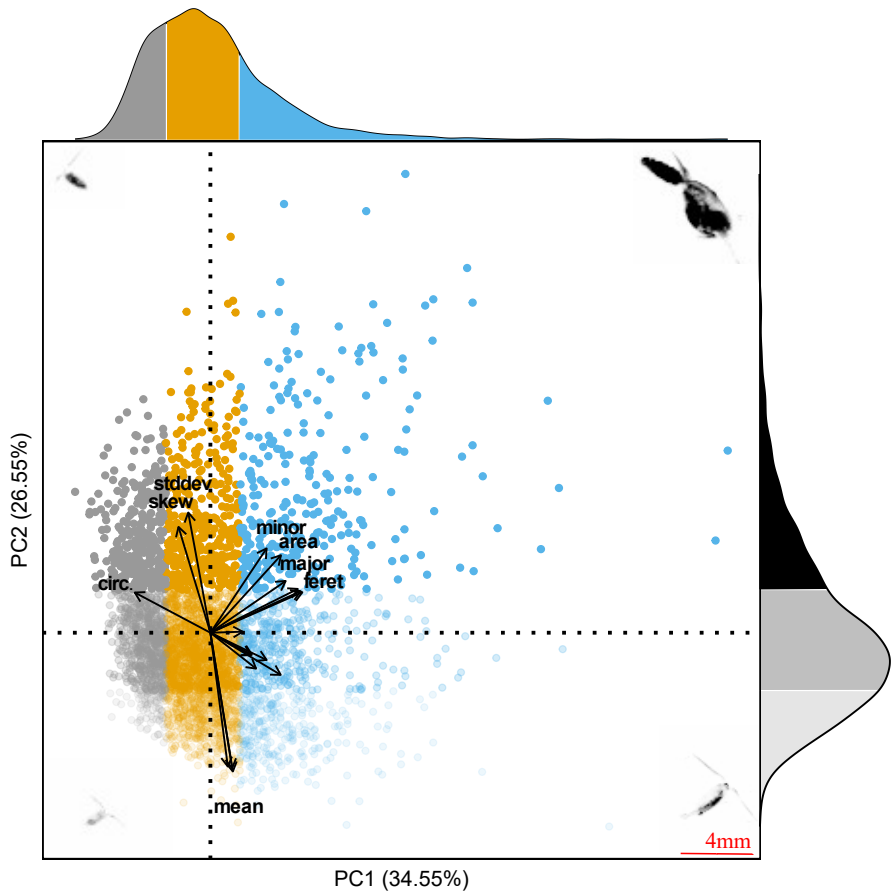


Figure 1: First two principal components of the morphospace. Proportion of variance explained by the two axis is 61.1%. Each point represents an individual copepod. The color and transparency of each point corresponds to the morphological groups based on percentile along each axis. Along PC1, grey corresponds to the low-group (<25th percentile), orange to the mid group (25th-75th percentiles), and blue to the high-group (75th percentile). Along PC2, low, mid, and high groups are distinguished by increasing opacity. Marginal distribution display the proportion of observations in each group. Representative vignettes of copepods are shown in the corners corresponding to their place in the morphospace. 4mm scale bar in the bottom right is shown for the vignettes.

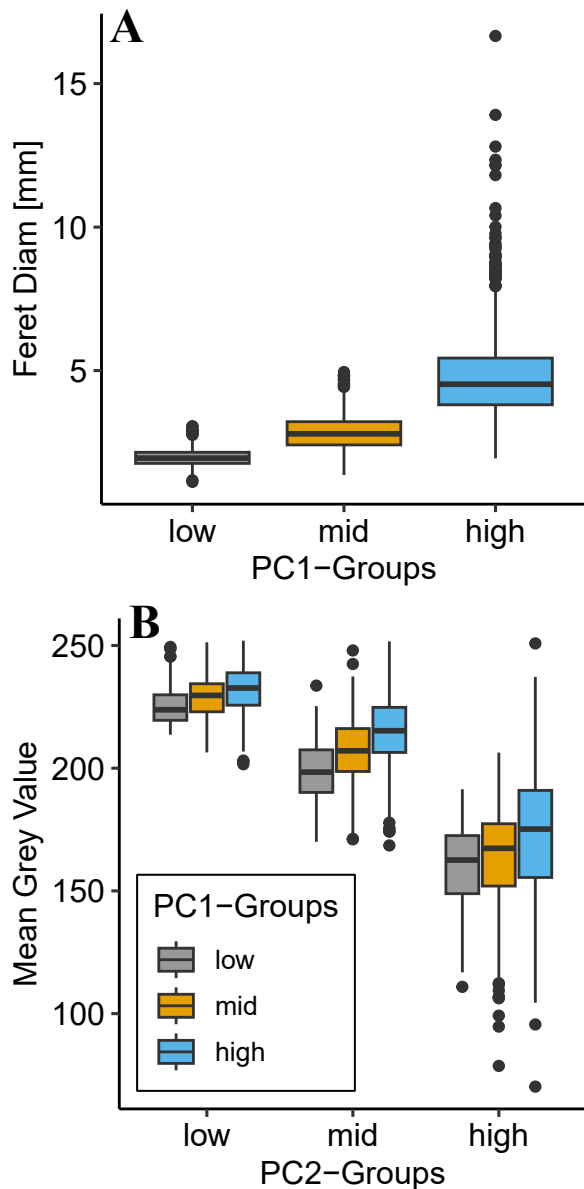


Figure 2: Comparison of morphological groups to relevant parameters. Groups were constructed along principal components with low as below 25th percentile, mid as 25th-50th percentile, and high as above 75th percentile. (A) PC1 groups are significantly different along feret diameter and display a clear trend for size. (B) PC2 groups are significantly different in terms of mean grey value. Note that a low mean grey value indicates a darker copepod.

³⁰⁷ upper mesopelagic (200m-300m). Then, there was a peak in average daytime
³⁰⁸ concentration in the depth bins in the mid-mesopelagic (400m-600m).

³⁰⁹ Weighted mean depth analysis

³¹⁰ The bin-constrained bootstrap approach provided a direct method to compare
³¹¹ DVM between groups. Size (PC1) had a clear effect on DVM magnitude. First,
³¹² for all PC1 groups, daytime WMD 95% bootstrapped confidence intervals (95%
³¹³ CIs) were deeper and non-overlapping with the nighttime 95% CIs (Figure 4).
³¹⁴ This indicates a clear DVM pattern. However, the differences in day and night
³¹⁵ CIs varied between morphological groups. All PC1 groups had a similar, over-
³¹⁶ lapping nighttime 95% CI in the lower epipelagic (~145m - ~200m). However,
³¹⁷ there was a clear difference in the depth of the daytime 95% CIs. The small
³¹⁸ (low PC1) group had the shallowest 95% CI (235.2m-296.0m). The mid PC1
³¹⁹ group's daytime 95% CI was slightly deeper (309.0m-347.3m). The large (high
³²⁰ PC1) group daytime 95% CI was even lower (352.3m-405.0m).

³²¹ When considering the influence of transparency (PC2) on DVM magnitude, we
³²² compared PC2 groups within their PC1 grouping. This approach was warranted
³²³ because of the tendency for size to have a slight effect on transparency (Figure
³²⁴ 2). At this level of comparison, there were several notable trends. For the
³²⁵ smaller copepods (low PC1), once the data were split into PC2 groups, the
³²⁶ wider 95% CIs indicate little to no DVM signal. Generally, the daytime 95%
³²⁷ CIs and nighttime 95% CIs are overlapping or near-overlapping (Figure 5A).
³²⁸ With mid-sized copepods, there was a clear DVM signal. However, all PC2

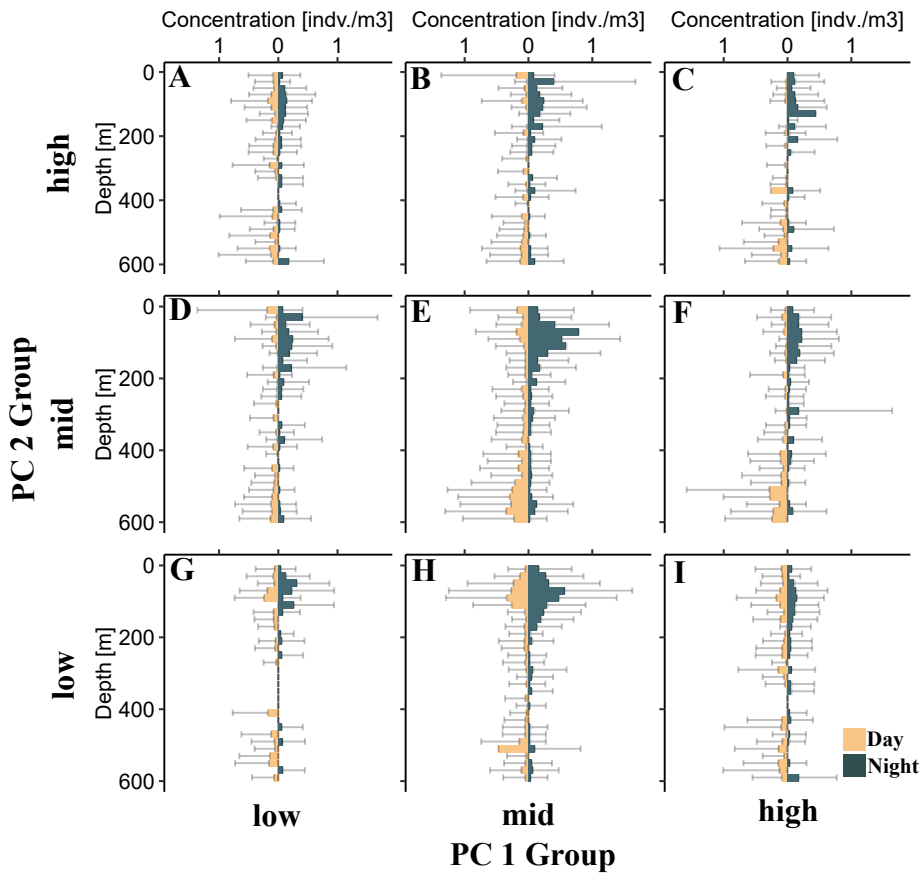


Figure 3: Average vertical profile of different copepod morphological groups. Bars display average concentration in a 20m depth bin. On each panel, left-side bars (tan) correspond to daytime while right-side (teal) bars correspond to nighttime. Standard deviation is shown for each 20m depth bin. Each panel corresponds to a morphological group along PC1 (size axis) and PC2 (transparency axis). (A) low PC1, high PC2; (B) mid PC1, high PC2; (C) high PC1, high PC2; (D) low PC1, mid PC2; (E) mid PC1, mid PC2; (F) high PC1, mid PC2; (G) low PC1, low PC2; (H) mid PC1, low PC2; (I) high PC1, low PC2

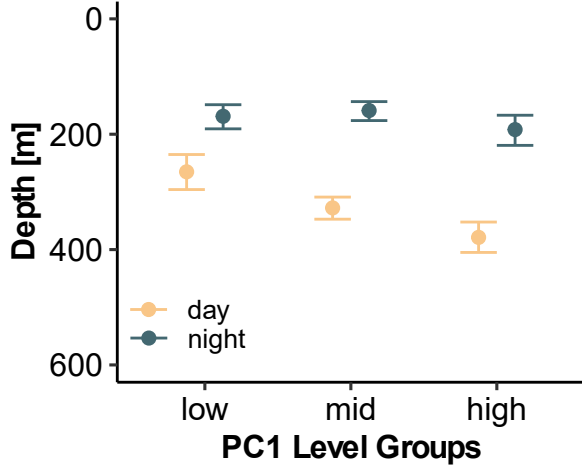


Figure 4: Mean bootstrapped weighted mean depth and 95% confidence intervals for copepods of different morphological groups. Low, mid, and high groups correspond to the different percentiles along PC1 from the morphospace. PC1 largely is explained by size metrics, with higher scores indicating a larger copepod.

329 groups appeared to have a similar DVM magnitude with each group's daytime
 330 95% CIs overlapping with each other (Figure 5B). There was a difference in
 331 DVM magnitude across PC2 groups within the largest copepods. The more
 332 transparent copepods (low PC2 group) showed no DVM signal, with a shallow
 333 daytime WMD. However, the darker copepods (mid and high PC2 groups) had
 334 deeper daytime WMDs (Figure 5c).

335 Discussion

336 Copepod morphospace & quantifying DVM

337 In this study, we built on methods for describing morphospaces from similar
 338 in-situ imaging studies (Vilgrain et al. 2021; Trudnowska et al. 2021; Sonnet

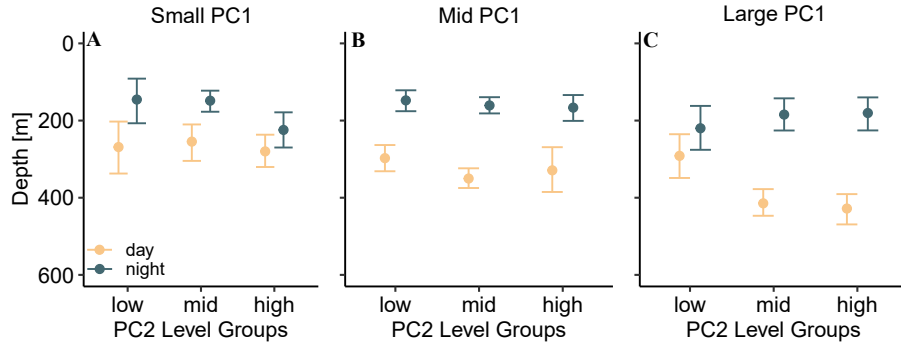


Figure 5: Mean bootstrapped weighted mean depth and 95% confidence intervals shown by copepod morphological groups along PC2 (transparency). Each panel represents a different size group of copepods (PC1 groups).

et al. 2022). The PCA-defined morphospace with the present data aligns well with the prior applications. Interestingly, the proportion of morphological variation explained by each axis in the morphospace defined on Arctic copepods by Vilgrain et al. (2021) is extremely similar to the morphospace axes in this study. This similarity is striking considering the vastly different copepod community compositions between the Arctic ocean and subtropical gyres (Soviadan et al. 2022). The similarity of morphospaces could also be an artifact of the similarity of input data. Given the UVP has a limited range of observable size classes (Picheral et al. 2010), only copepods above a certain size were fed into both PCAs. Alternatively, the similarity of studies suggest that copepod morphological variation might be well described by these two primary axes. (Sonnet et al. 2022) used phytoplankton images to investigate how a morphospace could be used to evaluate community composition changes over time. Comparisons of copepod morphospaces across temporal and spatial scales may offer a useful metric for answering biogeographic and ecological questions.

354 While the UVP provides some methodological challenges to quantifying DVM,
355 the pattern of DVM described in this study is consistent with the commonly
356 observed nocturnal DVM pattern (Bianchi and Mislan 2016; Bandara et al.
357 2021). The average vertical profiles display a clear day/night difference (Figure
358 3). However, in each 20m depth bin there was large variation, often exceeding
359 the average concentration. This large variation was expected. There can be con-
360 siderable variation between UVP estimates of zooplankton abundance (Barth
361 and Stone 2022). Additionally, in this study we pooled casts across multiple
362 seasons. Variability in copepod DVM has been described across seasons (Whit-
363 more and Ohman 2021). However, in the Sargasso Sea, while there is seasonal
364 variation in DVM biomass (Behrenfeld 2014), there is no record of variation
365 in DVM magnitude. Other studies describing DVM in the region have also
366 pooled across seasons using net data (Ivory et al. 2019). Thus, while pooling
367 across seasons may have introduced some variability in our WMD estimates,
368 the DVM signal was still well described by the UVP. Previous studies using in-
369 situ imaging have also noted a signal of DVM with copepods (Pan et al. 2018;
370 Whitmore and Ohman 2021). Yet due to small and uneven sampling, it can be
371 a challenge to quantify DVM using in-situ imaging. As presented in this paper,
372 bin-constrained bootstrapping offers a robust method to quantify WMD and
373 investigate DVM hypotheses.

³⁷⁴ **Morphological variation in DVM**

³⁷⁵ The results presented in this study provide new perspective on how traits influ-
³⁷⁶ ence DVM patterns. Consistent with the size-based hypothesis (H1), we docu-
³⁷⁷ mented a clear effect in which larger copepods migrated further. This finding
³⁷⁸ is consistent with several studies which have documented a size-dependent rela-
³⁷⁹ tionship for copepod DVM (Ohman and Romagnan 2016; Aarflot et al. 2019;
³⁸⁰ Pinti et al. 2019). Ohman and Romagnan (2016) noted that moderate-size
³⁸¹ copepods had the largest migrations. While this may seem contradictory to
³⁸² the present study, the difference between study systems needs be taken into
³⁸³ account. The copepods described in the large (high PC1) group had a mean
³⁸⁴ feret diameter of nearly 5mm. Conversely, in Ohman and Romagnan (2016)'s
³⁸⁵ study the "moderate" copepods ranged from 4mm-6mm.

³⁸⁶ The transparency-based hypothesis (H2) was only supported by patterns within
³⁸⁷ the large copepod group. The large but more transparent copepods (low PC2,
³⁸⁸ high PC1) did not have a detectable DVM signal. Yet the darker copepods (mid
³⁸⁹ and high PC2) had a large DVM signal. It should be noted that the grey-value
³⁹⁰ recorded by the UVP may be indicative of many features which influence cope-
³⁹¹ pod pigmentation, including pigmentation, egg-sacs and gut contents (Vilgrain
³⁹² et al. 2021). Thus, while our observation is consistent with both the predator-
³⁹³ avoidance and the hunger-satiation hypotheses, we cannot distinguish exactly
³⁹⁴ why the large, more transparent copepods do not migrate. One possibility is
³⁹⁵ that these copepods have empty gut contents, and thus are less transparent

396 and motivated to feed near the surface. However it is also plausible that the
397 difference in transparency is driven by taxonomic differences in pigmentation.
398 UVP images of copepods are generally unidentifiable to higher taxonomic reso-
399 lution. However, it is likely that the majority of copepod images were Calanoida,
400 which are consistently reported as the dominant copepod group in the Sargasso
401 Sea (Deevey and Brooks 1977; Ivory et al. 2019; Blanco-Bercial 2020). Addi-
402 tionally, a long-term analysis of net-collected data reported only Calanoida to
403 show a significant DVM signal (Ivory et al. 2019). However, within this group,
404 there is extreme diversity (Deevey and Brooks 1977; Blanco-Bercial 2020). In
405 a metabarcoding study of the epipelagic mesozooplankton community, Blanco-
406 Bercial (2020) reported *Pleuromamma spp.*, Euchaetidae, and Eucalanoidae to
407 show higher nighttime relative abundance. Alternatively, Calanidae were de-
408 scribed to occupy the surface waters at daytime. Thus, while the present study
409 cannot make direct conclusions as to taxonomic variation, it is likely a driving
410 factor in DVM variability across the observed morphological groups.
411 Hays (2003) described that copepod pigmentation could explain increased DVM
412 with small (<1mm) copepods. Thus it was surprising that there was no effect
413 of transparency on DVM magnitude in the smaller morphology group. One
414 possibility is that the small, transparent copepods were not well sampled by the
415 UVP (Figure 2). Due to the conservative nature of the bootstrapping WMD
416 approach utilized in this study, sampling deficits would broaden the 95% WMD
417 CI's, reducing the ability to resolve trends. However, there is no observable
418 trend to suggest the lack of DVM signal is simply a methodological artifact.

419 Alternatively, there are several possible explanations for why there is no effect
420 of transparency for the smaller copepod morphological groups. First, it should
421 be noted that while both the small-sized (low PC1) and mid-sized (mid-PC1)
422 group showed no variation in DVM patterns across PC2, the mid-sized group
423 consistently showed a strong DVM signal while the small-sized group did not.
424 Amongst the small-sized group, there was little observable DVM across all trans-
425 parency groupings. It may be that these copepods have a low visual-predator
426 risk regardless of their transparency level. Ohman and Romagnan (2016)'s study
427 in the California Current observed that the smallest copepods (<1.5mm) dis-
428 played no DVM signal. While these copepods may have reduced predator risk,
429 it may also be that they simply are weaker swimmers and cannot reasonably
430 migrate as large of distances as bigger copepods can.

431 The mid-sized copepods display a clear DVM signal across all transparency
432 groupings. This suggests that mid-sized copepods do not relieve their predation
433 risk through increased transparency. This is counterintuitive to the observation
434 that the large, transparent copepods have a reduced DVM signal. Additionally
435 the transparent, mid-sized copepods migrating while the transparent, large ones
436 do not, directly contradicts the predator-avoidance hypothesis. It is worth not-
437 ing that DVM behavior can also vary greatly across species. Within migrating
438 nekton, there has been mixed support described for the hunger-satiation hy-
439 pothesis, depending on taxa (Bos et al. 2021). Thus again it may be taxonomic
440 variation which can explain deviations in expected DVM patterns. Additionally,
441 other mechanisms influencing DVM, aside from top-down factors may be at

play. Williamson et al. (2011) provides support for the transparency-regulator hypothesis of DVM, which suggests both top-down factors and environmental factors such as UV-radiation influence DVM behavior. In the Sargasso Sea, there is extreme water clarity which would suggest UV-radiation may play a role in DVM behavior. However, none of our findings suggest that more pigmented copepods migrate less than transparent ones, regardless of size. Yet, across all copepod morphological groups, abundances were highest in the mid-to-lower mesopelagic and low in the surface layers (Figure 2). Thus the copepods imaged in this study are likely already at layers below where UV damage is a major factor. Furthermore, the deep chlorophyll-a maximum regularly extended into low epipelagic (Supplemental Figure S2), providing sufficient food where UV irradiance is low. Nonetheless, while UV may not be a primary factor, the notion that there are multiple factors influencing DVM should be considered.

Conclusion

Overall, our results reveal a complex dynamic between copepod traits and DVM behavior. This study provided new insight into the DVM dynamics in oligotrophic gyres. While many studies have established size as a major trait influencing DVM, investigations into other traits are more limited. Here, we support the prevailing notion that size has large consequences for DVM behavior. We also show that transparency has an effect on DVM for some size groups. However, determining exactly which drivers determine why copepods with different traits undergo diel vertical migration remains elusive. While these findings

464 are largely consistent with the predator-avoidance hypothesis and prevailing
465 DVM theory, they highlight the need for more detailed analyses. As plank-
466 ton in-situ imaging tools are used more commonly by oceanographers, larger
467 datasets will facilitate new investigations. Additionally, improved resolution
468 of sampling tools may better determine taxonomic variation. Collaborations
469 between oceanographers, plankton ecologists, and visual ecologists may better
470 resolve how traits influence trade-offs in DVM behavior. Understanding these
471 dynamics will be critical to predicting changes with a changing ocean.

472 **Acknowledgements**

473 Field work for this project was supported by the Bermuda Atlantic Time Series
474 Study through NSF OCE 1756105 & NSF OCE 1756312. We would also like
475 to thank the BATS research technicians, marine technicians, and crew of the
476 R/V Atlantic Explorer. Dr. Ryan Rykaczewski assisted with the initial set-up
477 of the UVP. Dr. Leo Blanco-Bercial and Dr. Amy Maas both valuable insight
478 and guidance on the analysis.

479 ***Data availability statement***

480 All data used in this project are hosted on Ecopart ([https://ecopart.obs-vlfr.](https://ecopart.obs-vlfr.fr/)
481 [fr/](https://ecopart.obs-vlfr.fr/)). Data in its raw form can be accessed from their portal. However, all
482 summary and intermediate data products, as well as code, are publicly available
483 on GitHub (https://github.com/TheAlexBarth/DVM_Migration-Morphology).

484 Intermediate data products are formatted as R Data Structure objects, other
485 formats are available on request.

486 **References**

- 487 Aarflot, J. M., D. L. Aksnes, A. F. Opdal, H. R. Skjoldal, and Ø. Fiksen.
488 2019. Caught in broad daylight: Topographic constraints of zooplankton depth distributions. *Limnology and Oceanography* **64**: 849–859.
489 doi:[10.1002/lno.11079](https://doi.org/10.1002/lno.11079)
- 490 Aksnes, D. L., and A. C. W. Utne. 1997. A revised model of visual range in
491 fish. *Sarsia* **82**: 137–147. doi:[10.1080/00364827.1997.10413647](https://doi.org/10.1080/00364827.1997.10413647)
- 492 Archibald, K. M., D. A. Siegel, and S. C. Doney. 2019. Modeling the
493 Impact of Zooplankton Diel Vertical Migration on the Carbon Export
494 Flux of the Biological Pump. *Global Biogeochemical Cycles* **33**: 181–199.
495 doi:[10.1029/2018GB005983](https://doi.org/10.1029/2018GB005983)
- 496 Atkinson, A., P. Ward, R. Williams, and S. A. Poulet. 1992. Diel vertical
497 migration and feeding of copepods at an oceanic site near South Georgia.
498 Marine Biology **113**: 583–593. doi:[10.1007/BF00349702](https://doi.org/10.1007/BF00349702)
- 499 Bandara, K., Ø. Varpe, R. Ji, and K. Eiane. 2019. Artificial evolution of
500 behavioral and life history strategies of high-latitude copepods in response
501 to bottom-up and top-down selection pressures. *Progress in Oceanography*
502 **173**: 134–164. doi:[10.1016/j.pocean.2019.02.006](https://doi.org/10.1016/j.pocean.2019.02.006)
- 503 Bandara, K., Ø. Varpe, L. Wijewardene, V. Tverberg, and K. Eiane. 2021.
504 Two hundred years of zooplankton vertical migration research. *Biological*

- 506 Reviews **96**: 1547–1589. doi:[10.1111/brv.12715](https://doi.org/10.1111/brv.12715)
- 507 Barth, A., and J. Stone. 2022. Comparison of an in situ imaging device and
508 net-based method to study mesozooplankton communities in an oligotrophic
509 system. Frontiers in Marine Science **9**.
- 510 Behrenfeld, M. J. 2014. Climate-mediated dance of the plankton. Nature Cli-
511 mate Change **4**: 880–887. doi:[10.1038/nclimate2349](https://doi.org/10.1038/nclimate2349)
- 512 Behrenfeld, M. J., P. Gaube, A. Della Penna, and others. 2019. Global satellite-
513 observed daily vertical migrations of ocean animals. Nature **576**: 257–261.
514 doi:[10.1038/s41586-019-1796-9](https://doi.org/10.1038/s41586-019-1796-9)
- 515 Bianchi, D., and K. a. S. Mislan. 2016. Global patterns of diel vertical migration
516 times and velocities from acoustic data. Limnology and Oceanography **61**:
517 353–364. doi:[10.1002/lno.10219](https://doi.org/10.1002/lno.10219)
- 518 Blanco-Bercial, L. 2020. Metabarcoding analyses and seasonality of the zoo-
519 plankton community at BATS. Frontiers in Marine Science **7**.
- 520 Bos, R. P., T. T. Sutton, and T. M. Frank. 2021. State of satiation partially
521 regulates the dynamics of vertical migration. Frontiers in Marine Science **8**.
- 522 Brierley, A. S. 2014. Diel vertical migration. Current Biology **24**: R1074–R1076.
523 doi:[10.1016/j.cub.2014.08.054](https://doi.org/10.1016/j.cub.2014.08.054)
- 524 Cohen, J. H., and R. B. Forward Jr. 2009. Zooplankton diel vertical migration:
525 a review of proximate control, p. 77–110. In.
- 526 Deevey, G. B., and A. L. Brooks. 1977. Copepods of the sargasso sea off
527 bermuda: Species composition, and vertical and seasonal distribution be-
528 tween the surface and 2000 m. Bulletin of Marine Science **27**: 256–291.

- 529 Enright, J. T. 1977. Diurnal vertical migration: Adaptive significance and tim-
530 ing. Part 1. Selective advantage: A metabolic model1. Limnology and
531 Oceanography **22**: 856–872. doi:[10.4319/lo.1977.22.5.0856](https://doi.org/10.4319/lo.1977.22.5.0856)
- 532 Ewald, W. F. 1912. On artificial modification of light reactions and the influence
533 of electrolytes on phototaxis. Journal of Experimental Zoology **13**: 591–612.
534 doi:[10.1002/jez.1400130405](https://doi.org/10.1002/jez.1400130405)
- 535 Gorsky, G., M. D. Ohman, M. Picheral, and others. 2010. Digital zooplankton
536 image analysis using the ZooScan integrated system. Journal of Plankton
537 Research **32**: 285–303. doi:[10.1093/plankt/fbp124](https://doi.org/10.1093/plankt/fbp124)
- 538 Hays, G. C. 2003. [A review of the adaptive significance and ecosystem conse-](#)
539 [quences of zooplankton diel vertical migrations](#). Springer Netherlands. 163–
540 170.
- 541 Hays, G. C., C. A. Proctor, A. W. G. John, and A. J. Warner. 1994. Inter-
542 specific differences in the diel vertical migration of marine copepods: The
543 implications of size, color, and morphology. Limnology and Oceanography
544 **39**: 1621–1629. doi:[10.4319/lo.1994.39.7.1621](https://doi.org/10.4319/lo.1994.39.7.1621)
- 545 Ivory, J. A., D. K. Steinberg, and R. J. Latour. 2019. Diel, seasonal, and inter-
546 annual patterns in mesozooplankton abundance in the sargasso sea. ICES
547 Journal of Marine Science **76**: 217–231. doi:[10.1093/icesjms/fsy117](https://doi.org/10.1093/icesjms/fsy117)
- 548 Kelly, T. B., P. C. Davison, R. Goericke, M. R. Landry, M. D. Ohman, and M.
549 R. Stukel. 2019. [The importance of mesozooplankton diel vertical migration](#)
550 [for sustaining a mesopelagic food web](#). Frontiers in Marine Science **6**.
- 551 Kessler, K., R. S. Lockwood, C. E. Williamson, and J. E. Saros. 2008. Vertical

552 distribution of zooplankton in subalpine and alpine lakes: Ultraviolet radi-
553 ation, fish predation, and the transparency-gradient hypothesis. Limnology
554 and Oceanography **53**: 2374–2382. doi:[10.4319/lo.2008.53.6.2374](https://doi.org/10.4319/lo.2008.53.6.2374)

555 Lampert, W. 1989. The adaptive significance of diel vertical migration of zoo-
556 plankton. Functional Ecology **3**: 21–27. doi:[10.2307/2389671](https://doi.org/10.2307/2389671)

557 Liu, Y., J. Guo, Y. Xue, C. Sangmanee, H. Wang, C. Zhao, S. Khokiattiwong,
558 and W. Yu. 2022. Seasonal variation in diel vertical migration of zooplank-
559 ton and micronekton in the andaman sea observed by a moored ADCP.
560 Deep Sea Research Part I: Oceanographic Research Papers **179**: 103663.
561 doi:[10.1016/j.dsr.2021.103663](https://doi.org/10.1016/j.dsr.2021.103663)

562 Maas, A. E., L. Blanco-Bercial, A. Lo, A. M. Tarrant, and E. Timmins-
563 Schiffman. 2018. Variations in copepod proteome and respiration rate in
564 association with diel vertical migration and circadian cycle. The Biological
565 Bulletin **235**: 30–42. doi:[10.1086/699219](https://doi.org/10.1086/699219)

566 McLaren, I. A. 1963. Effects of temperature on growth of zooplankton, and
567 the adaptive value of vertical migration. Journal of the Fisheries Research
568 Board of Canada **20**: 685–727. doi:[10.1139/f63-046](https://doi.org/10.1139/f63-046)

569 McLaren, I. A. 1974. Demographic strategy of vertical migration by a marine
570 copepod. The American Naturalist **108**: 91–102.

571 Ohman, M. D. 1990. The Demographic Benefits of Diel Vertical Migration by
572 Zooplankton. Ecological Monographs **60**: 257–281. doi:[10.2307/1943058](https://doi.org/10.2307/1943058)

573 Ohman, M. D. 2019. A sea of tentacles: optically discernible traits resolved from
574 planktonic organisms in situ H. Browman [ed.]. ICES Journal of Marine

- 575 Science **76**: 1959–1972. doi:[10.1093/icesjms/fsz184](https://doi.org/10.1093/icesjms/fsz184)
- 576 Ohman, M. D., and J.-B. Romagnan. 2016. Nonlinear effects of body size and
577 optical attenuation on Diel Vertical Migration by zooplankton. Limnology
578 and Oceanography **61**: 765–770. doi:[10.1002/lo.10251](https://doi.org/10.1002/lo.10251)
- 579 Ohman, M. D., J. A. Runge, E. G. Durbin, D. B. Field, and B. Niehoff.
580 2002. On birth and death in the sea. Hydrobiologia **480**: 55–68.
581 doi:[10.1023/A:1021228900786](https://doi.org/10.1023/A:1021228900786)
- 582 Pan, J., F. Cheng, and F. Yu. 2018. The diel vertical migration of zooplankton
583 in the hypoxia area observed by video plankton recorder. IJMS Vol.47(07)
584 [July 2018].
- 585 Pearre, S. 2003. Eat and run? The hunger/satiation hypothesis in vertical
586 migration: history, evidence and consequences. Biological Reviews **78**: 1–
587 79. doi:[10.1017/S146479310200595X](https://doi.org/10.1017/S146479310200595X)
- 588 Picheral, M., S. Colin, and J.-O. Irisson. 2017. EcoTaxa, a tool for the taxo-
589 nomic classification of images.
- 590 Picheral, M., L. Guidi, L. Stemmann, D. M. Karl, G. Iddaoud, and G. Gorsky.
591 2010. The Underwater Vision Profiler 5: An advanced instrument for high
592 spatial resolution studies of particle size spectra and zooplankton. Limnology
593 and Oceanography: Methods **8**: 462–473. doi:[10.4319/lom.2010.8.462](https://doi.org/10.4319/lom.2010.8.462)
- 594 Pinti, J., T. Kiørboe, U. H. Thygesen, and A. W. Visser. 2019. Trophic in-
595 teractions drive the emergence of diel vertical migration patterns: A game-
596 theoretic model of copepod communities. Proceedings of the Royal Society
597 B: Biological Sciences **286**: 20191645. doi:[10.1098/rspb.2019.1645](https://doi.org/10.1098/rspb.2019.1645)

- 598 Ringelberg, J. 2009. Diel Vertical Migration of Zooplankton in Lakes and
599 Oceans: causal explanations and adaptive significances, Springer Science
600 & Business Media.
- 601 Robison, B. H., R. E. Sherlock, K. R. Reisenbichler, and P. R. McGill. 2020.
602 [Running the gauntlet: Assessing the threats to vertical migrators](#). Frontiers
603 in Marine Science **7**.
- 604 Schnetzer, A., and D. K. Steinberg. 2002. Active transport of particu-
605 late organic carbon and nitrogen by vertically migrating zooplankton
606 in the Sargasso Sea. Marine Ecology Progress Series **234**: 71–84.
607 doi:[10.3354/meps234071](https://doi.org/10.3354/meps234071)
- 608 Siegel, D. A., T. DeVries, I. Cetinić, and K. M. Bisson. 2023. Quantifying
609 the ocean's biological pump and its carbon cycle impacts on global scales.
610 Annual Review of Marine Science **15**: null. doi:[10.1146/annurev-marine-040722-115226](https://doi.org/10.1146/annurev-marine-040722-115226)
- 612 Sonnet, V., L. Guidi, C. B. Mouw, G. Puggioni, and S.-D. Ayata. 2022. Length,
613 width, shape regularity, and chain structure: time series analysis of phy-
614toplankton morphology from imagery. Limnology and Oceanography **67**:
615 1850–1864. doi:[10.1002/lno.12171](https://doi.org/10.1002/lno.12171)
- 616 Soviadan, Y. D., F. Benedetti, M. C. Brandão, and others. 2022.
617 Patterns of mesozooplankton community composition and vertical
618 fluxes in the global ocean. Progress in Oceanography **200**: 102717.
619 doi:[10.1016/j.pocean.2021.102717](https://doi.org/10.1016/j.pocean.2021.102717)
- 620 Steinberg, D. K., C. A. Carlson, N. R. Bates, S. A. Goldthwait, L. P. Madin,

621 and A. F. Michaels. 2000. Zooplankton vertical migration and the active
622 transport of dissolved organic and inorganic carbon in the Sargasso Sea.
623 Deep Sea Research Part I: Oceanographic Research Papers **47**: 137–158.
624 doi:[10.1016/S0967-0637\(99\)00052-7](https://doi.org/10.1016/S0967-0637(99)00052-7)

625 Steinberg, D. K., C. A. Carlson, N. R. Bates, R. J. Johnson, A. F. Michaels,
626 and A. H. Knap. 2001. Overview of the US JGOFS Bermuda Atlantic
627 Time-series Study (BATS): a decade-scale look at ocean biology and biogeo-
628 chemistry. Deep Sea Research Part II: Topical Studies in Oceanography **48**:
629 1405–1447. doi:[10.1016/S0967-0645\(00\)00148-X](https://doi.org/10.1016/S0967-0645(00)00148-X)

630 Steinberg, D. K., and M. R. Landry. 2017. Zooplankton and the ocean carbon
631 cycle. Annual Review of Marine Science **9**: 413–444. doi:[10.1146/annurev-marine-010814-015924](https://doi.org/10.1146/annurev-marine-010814-015924)

632 Szeligowska, M., E. Trudnowska, R. Boehnke, A. M. Dąbrowska, K. Dragańska-
633 Deja, K. Deja, M. Darecki, and K. Błachowiak-Samołyk. 2021. The inter-
634 play between plankton and particles in the Isfjorden waters influenced by
635 marine- and land-terminating glaciers. Science of The Total Environment
636 **780**: 146491. doi:[10.1016/j.scitotenv.2021.146491](https://doi.org/10.1016/j.scitotenv.2021.146491)

637 Trudnowska, E., L. Lacour, M. Ardyna, A. Rogge, J. O. Irisson, A. M. Waite, M.
638 Babin, and L. Stemmann. 2021. Marine snow morphology illuminates the
639 evolution of phytoplankton blooms and determines their subsequent vertical
640 export. Nature Communications **12**: 2816. doi:[10.1038/s41467-021-22994-4](https://doi.org/10.1038/s41467-021-22994-4)

641 Turner, J. 2004. The importance of small planktonic copepods and their roles
642 in pelagic marine food webs.,

- 644 Vilgrain, L., F. Maps, M. Picheral, M. Babin, C. Aubry, J.-O. Irisson, and S.-D.
 645 Ayata. 2021. Trait-based approach using in situ copepod images reveals
 646 contrasting ecological patterns across an Arctic ice melt zone. Limnology
 647 and Oceanography **66**: 1155–1167. doi:[10.1002/lno.11672](https://doi.org/10.1002/lno.11672)
 648 Whitmore, B. M., and M. D. Ohman. 2021. Zooglider-measured association of
 649 zooplankton with the fine-scale vertical prey field. Limnology and Oceanog-
 650 raphy **66**: 3811–3827. doi:[10.1002/lno.11920](https://doi.org/10.1002/lno.11920)
 651 Williamson, C. E., J. M. Fischer, S. M. Bollens, E. P. Overholt, and J. K. Breck-
 652 enridge. 2011. Toward a more comprehensive theory of zooplankton diel
 653 vertical migration: Integrating ultraviolet radiation and water transparency
 654 into the biotic paradigm. Limnology and Oceanography **56**: 1603–1623.
 655 doi:[10.4319/lo.2011.56.5.1603](https://doi.org/10.4319/lo.2011.56.5.1603)
 656 Zaret, T. M., and J. S. Suffern. 1976. Vertical migration in zooplankton as a
 657 predator avoidance mechanism1. Limnology and Oceanography **21**: 804–813.
 658 doi:[10.4319/lo.1976.21.6.0804](https://doi.org/10.4319/lo.1976.21.6.0804)

659 Supplemental Information

	Dim.1	Dim.2	Dim.3	Dim.4
area	0.7115131	0.5137738	-0.1301928	0.3789753
circ.	-0.7627265	0.2665557	-0.3026239	0.3034329
elongation	0.4080632	-0.1487560	-0.7831847	-0.2965671
feret	0.9096148	0.2756948	-0.2479648	0.0082808

	Dim.1	Dim.2	Dim.3	Dim.4
fractal	0.8816770	0.2904962	-0.0440580	0.1793785
histcum1	0.2197180	-0.8987922	-0.0901744	0.3005361
major	0.7593652	0.3432489	-0.5115438	0.1498407
mean	0.2266145	-0.9201880	-0.0611832	0.2875560
median	0.1758116	-0.8872673	0.0657406	0.1668198
minor	0.5668215	0.5593596	0.2891461	0.4585166
perim.	0.9268957	0.2685898	0.0681774	0.1135716
perimferet	0.3251295	0.0068372	0.7989292	0.2111105
perimmajor	0.4183142	-0.1460583	0.8627707	-0.1389696
skew	-0.3216781	0.7017490	0.1514517	-0.1447764
stddev	-0.2234641	0.7971849	0.1531288	-0.3647663
symetriev	0.7091737	-0.2793593	-0.0605051	-0.5720602
symtrievc	0.5673730	-0.1807542	-0.2368157	-0.4811256
thickr	0.4609473	-0.2379533	0.5832035	-0.3954358

660 Supplemental Table S2. Loading scores for morphological factors on the PCA.

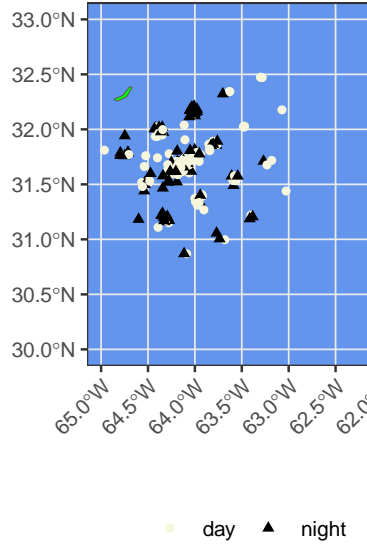


Figure 6: Supplemental Figure S1. Map of CTD Cast Deployments. Dark triangle points indicate night casts, tan circles indicate day casts.

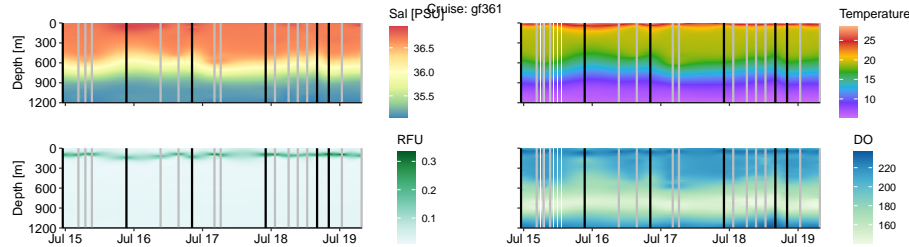


Figure 7: Supplemental Figure S2. Physical parameters across individual cruises. Vertical bars indicate CTD casts events with black indicating night and grey indicating day.

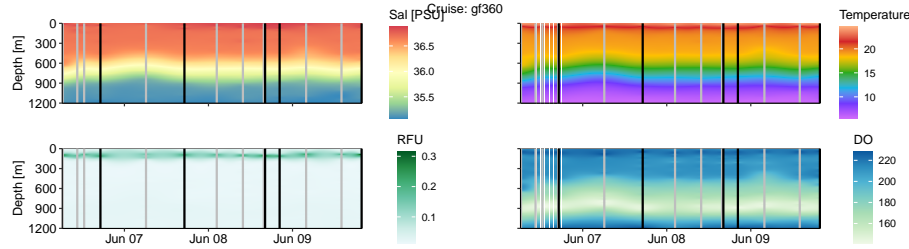


Figure 8: Supplemental Figure S2. Physical parameters across individual cruises. Vertical bars indicate CTD casts events with black indicating night and grey indicating day.

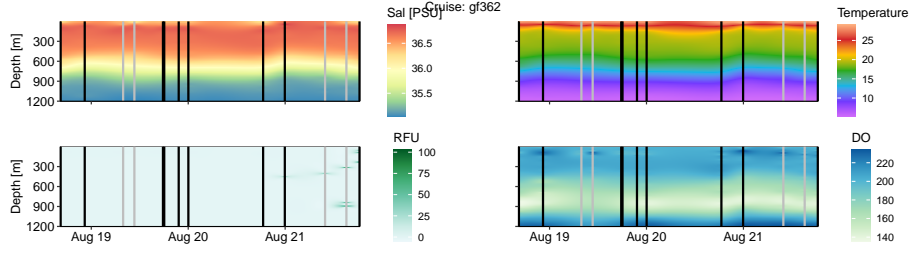


Figure 9: Supplemental Figure S2. Physical parameters across individual cruises. Vertical bars indicate CTD casts events with black indicating night and grey indicating day.

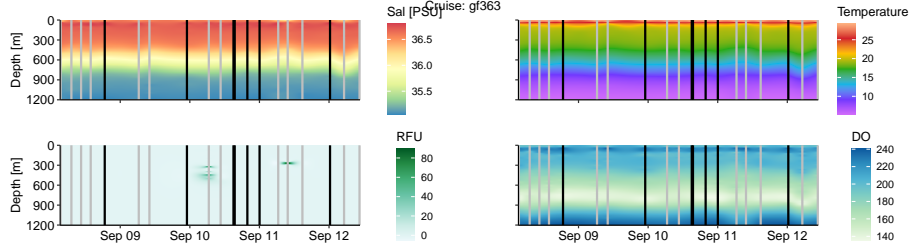


Figure 10: Supplemental Figure S2. Physical parameters across individual cruises. Vertical bars indicate CTD casts events with black indicating night and grey indicating day.

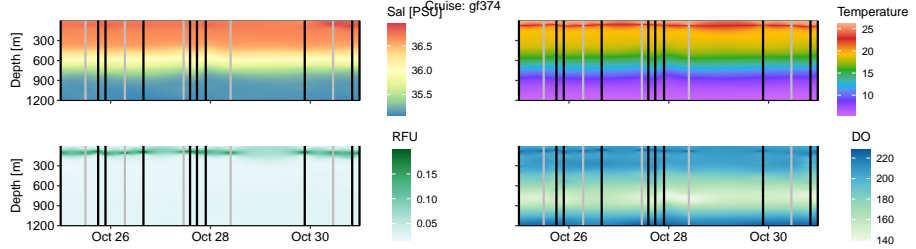


Figure 11: Supplemental Figure S2. Physical parameters across individual cruises. Vertical bars indicate CTD casts events with black indicating night and grey indicating day.

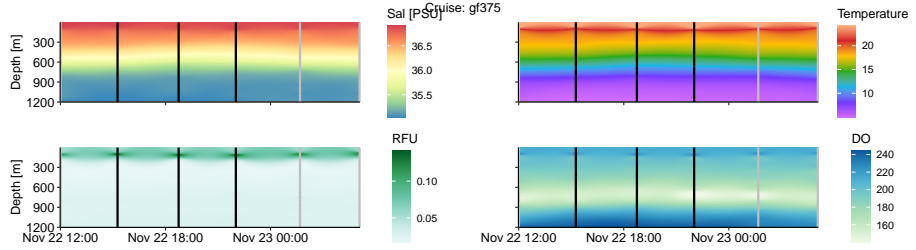


Figure 12: Supplemental Figure S2. Physical parameters across individual cruises. Vertical bars indicate CTD casts events with black indicating night and grey indicating day.

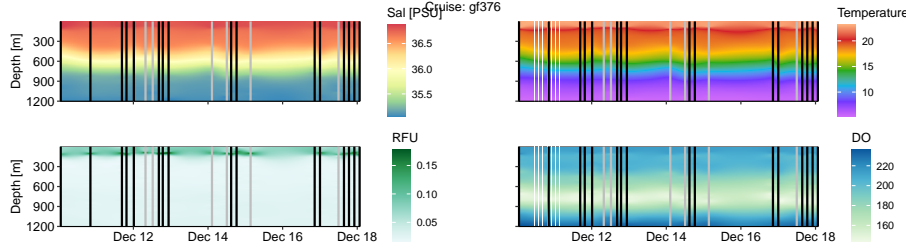


Figure 13: Supplemental Figure S2. Physical parameters across individual cruises. Vertical bars indicate CTD casts events with black indicating night and grey indicating day.

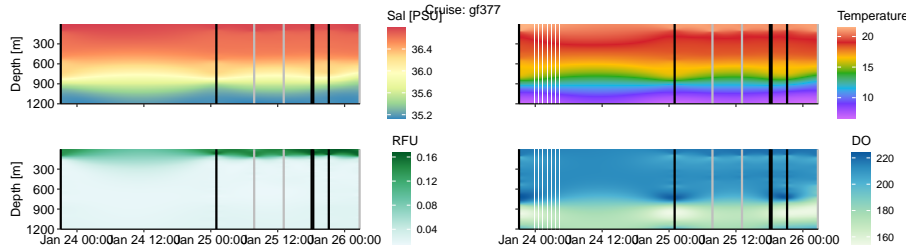


Figure 14: Supplemental Figure S2. Physical parameters across individual cruises. Vertical bars indicate CTD casts events with black indicating night and grey indicating day.

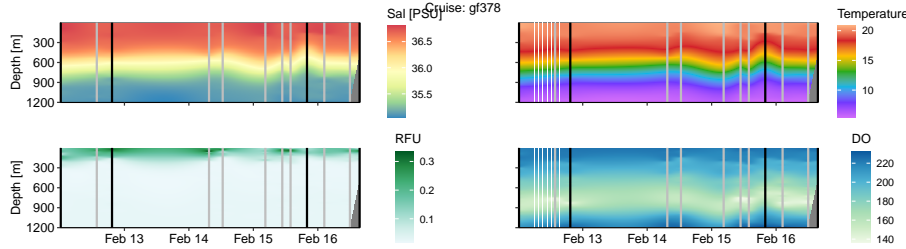


Figure 15: Supplemental Figure S2. Physical parameters across individual cruises. Vertical bars indicate CTD casts events with black indicating night and grey indicating day.

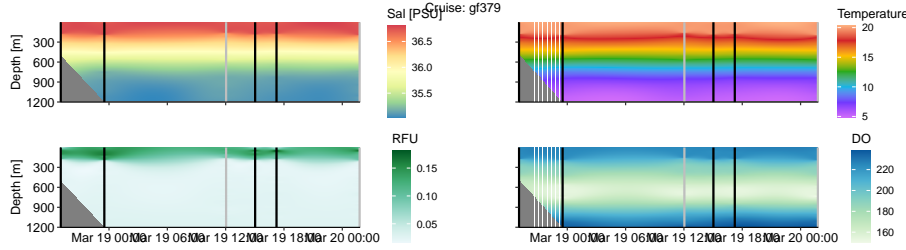


Figure 16: Supplemental Figure S2. Physical parameters across individual cruises. Vertical bars indicate CTD casts events with black indicating night and grey indicating day.

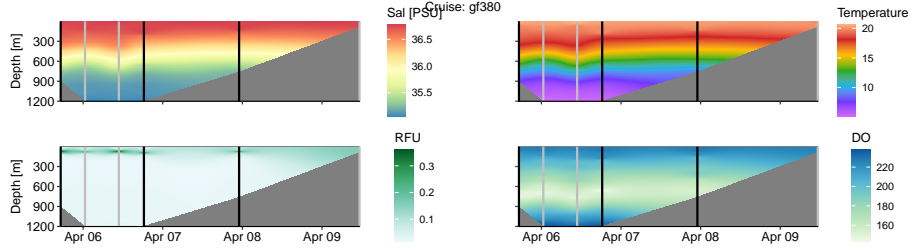


Figure 17: Supplemental Figure S2. Physical parameters across individual cruises. Vertical bars indicate CTD casts events with black indicating night and grey indicating day.

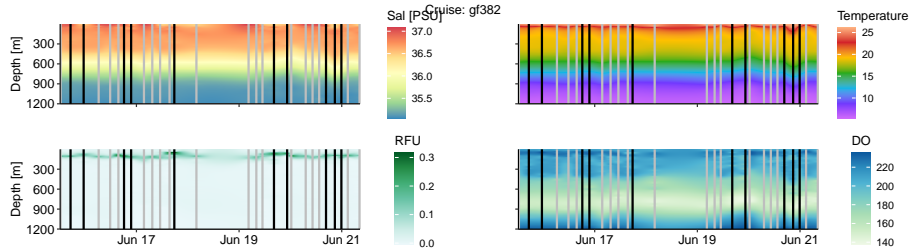


Figure 18: Supplemental Figure S2. Physical parameters across individual cruises. Vertical bars indicate CTD casts events with black indicating night and grey indicating day.

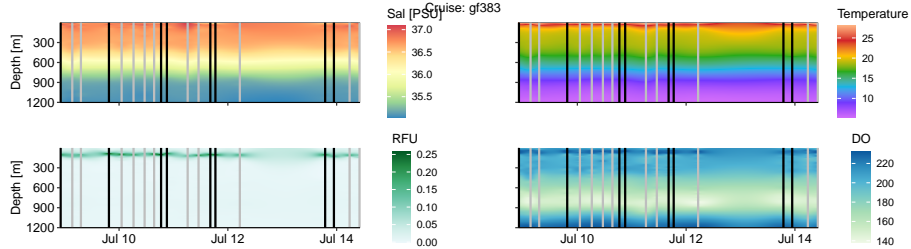


Figure 19: Supplemental Figure S2. Physical parameters across individual cruises. Vertical bars indicate CTD casts events with black indicating night and grey indicating day.

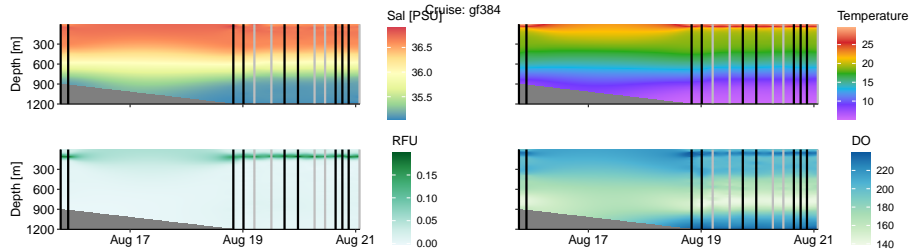


Figure 20: Supplemental Figure S2. Physical parameters across individual cruises. Vertical bars indicate CTD casts events with black indicating night and grey indicating day.

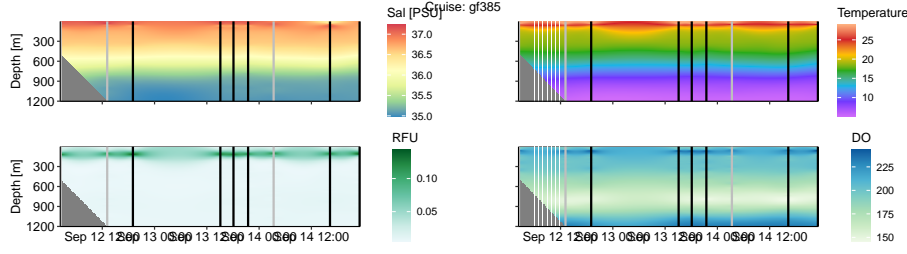


Figure 21: Supplemental Figure S2. Physical parameters across individual cruises. Vertical bars indicate CTD casts events with black indicating night and grey indicating day.

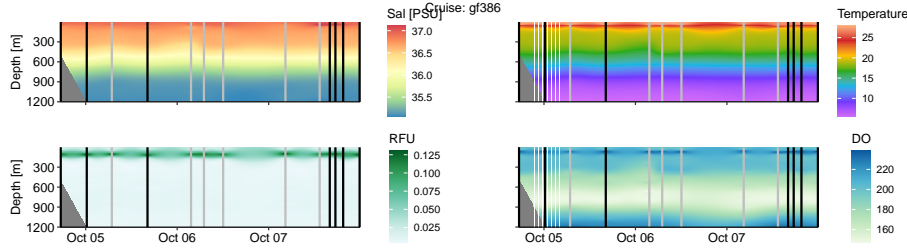


Figure 22: Supplemental Figure S2. Physical parameters across individual cruises. Vertical bars indicate CTD casts events with black indicating night and grey indicating day.

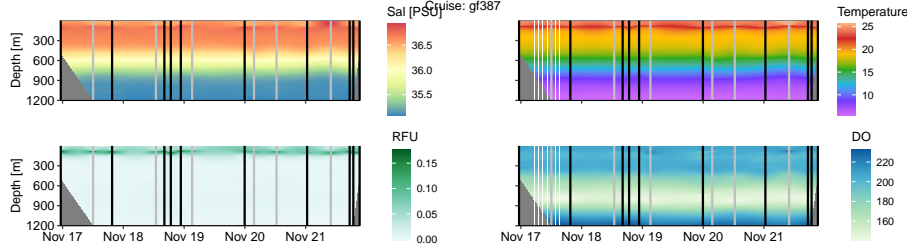


Figure 23: Supplemental Figure S2. Physical parameters across individual cruises. Vertical bars indicate CTD casts events with black indicating night and grey indicating day.

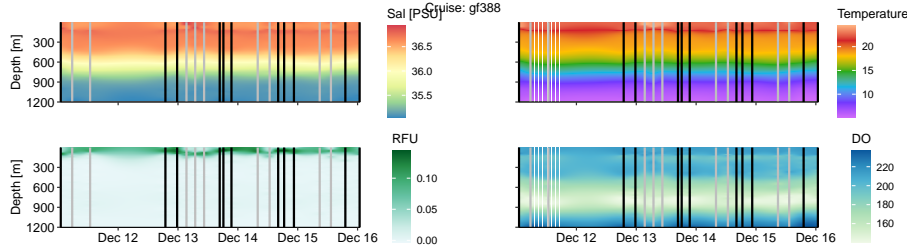


Figure 24: Supplemental Figure S2. Physical parameters across individual cruises. Vertical bars indicate CTD casts events with black indicating night and grey indicating day.

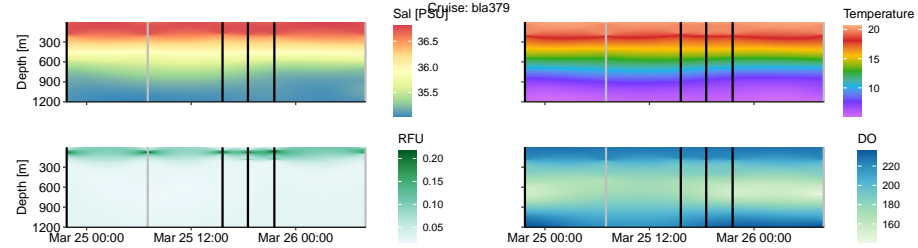


Figure 25: Supplemental Figure S2. Physical parameters across individual cruises. Vertical bars indicate CTD casts events with black indicating night and grey indicating day.

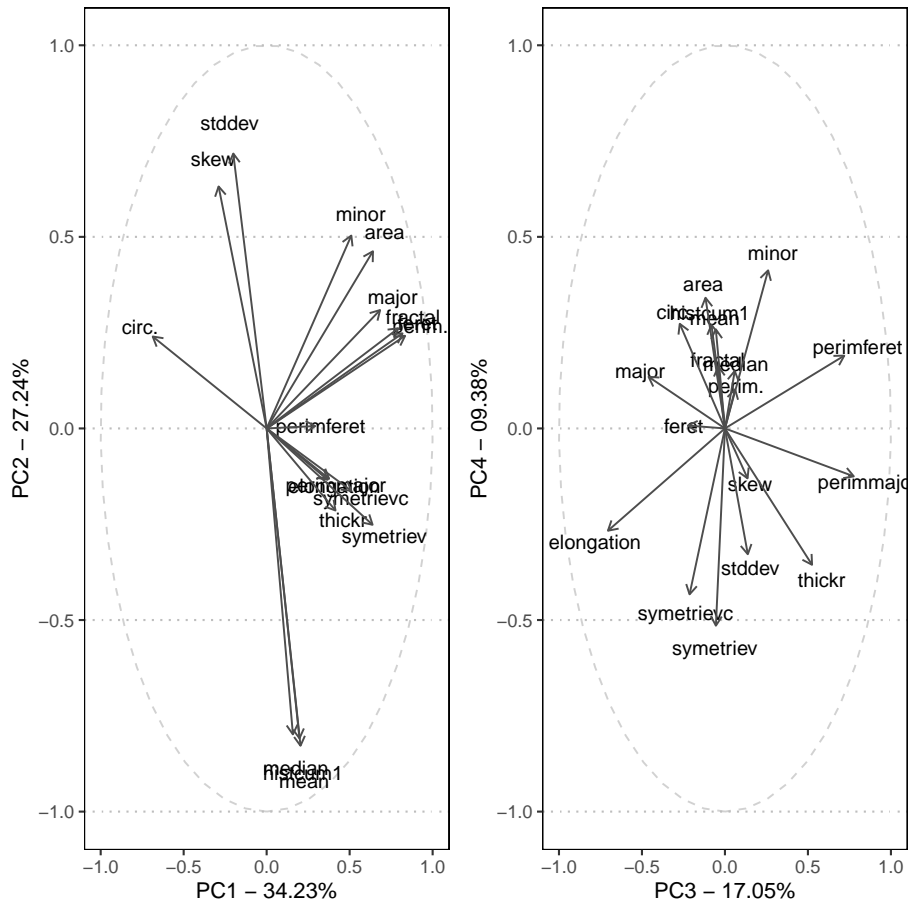


Figure 26: Supplemental Figure S3. PCA plot with major loading variables plotted.